23rd ABCM International Congress of Mechanical Engineering
December 6-11, 2015, Rio de Janeiro, RJ, Brazil

STRUCTURAL ANALYSIS OF A FORMULA SAE CHASSIS UNDER ROLLOVER LOADS

Felipe Azevedo Canut
University of Brasília, Faculty of Technology, Department of Mechanical Engineering
felipe.canut@gmail.com

Lucival Malcher
University of Brasília, Faculty of Technology, Department of Mechanical Engineering
malcher@unb.br

Antonio Manuel Dias Henriques
University of Brasília, Faculty of Technology, Department of Mechanical Engineering
henriques@unb.br

Abstract. *The purpose of Formula SAE is to provide students an opportunity to design, fabricate, and then demonstrate the performance of a prototype racecar. The study presents the finite element analysis of a formula SAE chassis under loads presented on the Formula SAE rules, aiming to ensure the minimum stiffness of the roll hoops and the driver's safety. The von Mises constitutive model was used in the simulations to predict the roll hoop's displacements. In addition, experimental displacements were measured on a test table through a load application. Numerical and experimental displacements are compared in order to validate the finite element analysis. The different tests showed that the chassis in study doesn't present the proper stiffness. Finally, the simulation and experimental methods are discussed and geometry improvements are proposed in order to ensure the driver's safety.*

1. INTRODUCTION

Both in racing as in the streetcars, the chassis is a critical component to performance and safety. For good performance, the chassis must be perfectly rigid, when compared to suspension and be as light as possible (Milliken and Milliken, 1995). The chassis is also responsible for resisting collisions and rollover loads, ensuring the vehicle's occupants safety.

The modern chassis are extremely complex structures to be analyzed, and analyzing them by classical analytical methods is a nearly an impossible mission. For this kind of analysis, approximate numerical methods are used, which can be applied to any structure, regardless of their shape or loading conditions. With a good numerical model, the number of prototypes constructed can be reduced, making the analysis cheaper. The computational cost of an analysis made by finite element methods depends on the degree of the mesh's refinement and the model's boundary conditions.

This paper aims to analyze the UnB formula SAE team's chassis when the loads imposed by FSAE's rules are applied, simulating a rollover situation and compare numerical and experimental obtained results. Numerical analysis was done by finite element method, through Abaqus v6.10 software, and the experimental analysis was performed on a test bench at the University of Brasilia, campus Gama. Since the numerical analysis is consistent with the experimental results, it is possible to propose improvements in the chassis' design without the need to build new prototypes.

The purpose of numerical analysis is to determine the critical parts of the chassis, and to verify if the deflections are not exceeded. The points listed as critical for analysis are measured by a coordinate measurements machine on the experimental test. The results of the experimental analysis serve to validate the numerical model proposed.

2. THEORETICAL ASPECTS

2.1 Vehicle structure

According to FSAE rules, the vehicle's structure must include two roll hoops (Main and Front Hoop) and their supporters (Main Hoop Bracing and the Main Hoop Bracing supports), front bracket for fixing the impact attenuator (Front Bulkhead), and side impact structure. These structures can be seen in Fig. 1.

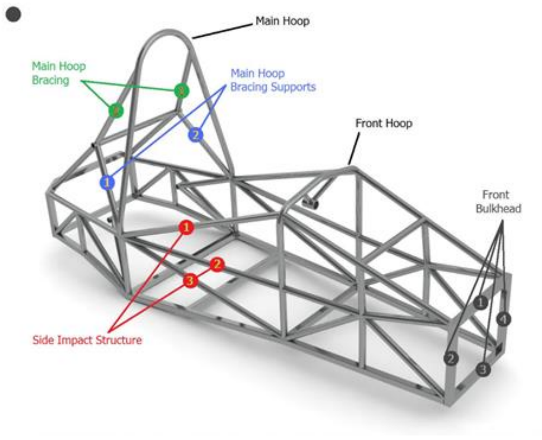

Figure 1. Primary structures (FSAE Rules, 2014).

The main function of the roll hoops (Main and Front Hoop) is to guarantee the pilot's protection in case of rollover. The driver's head and hands must not touch the ground in any rollover attitude. According to FSAE rules, the driver must meet the helmet clearance requirements, as shown in Fig. 2.

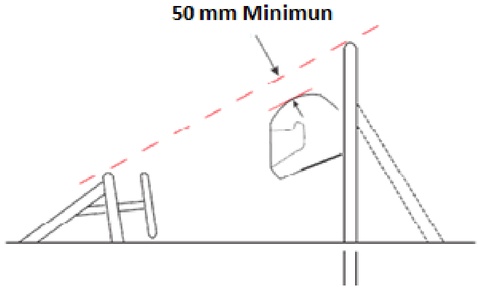

Figure 2. Helmet clearence (FSAE Rules, 2014 - modified).

2.2 Elastic-plastic constitutive model

According to Souza et al. (2008), some important properties can be identified in the uniaxial traction test, shown in Fig. 3. A range of stresses can be considered as purely elastic (elastic domain) if there is no evolution of permanent strains. The elastic domain in delimited by the so-called yield stress. If the material is loaded beyond that limit, then permanent strain, or plastic strain, is observed. For fragile materials, such as concrete or glass, the elastic domain corresponds to almost all strain before the failure. Ductile material may have a much bigger plastic strain under ultimate loads condition.

The mathematical theory of plasticity used in this study has the objective to provide a model capable of describing, with the sufficient accuracy, the behavior of the material under conditions beyond the yield stress.

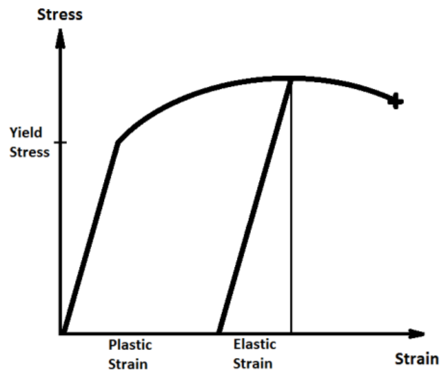

Figure 3. Stress-strain typical curve for ductile materials.

To understand the concepts involved in the definition of a constitutive model, is necessary presenting some preliminary definitions. The so-called stress tensor σ can be written as the sum of volumetric and deviatoric contributions (Souza et al. 2008), as shown in Eq (1).

$$\boldsymbol{\sigma} = \boldsymbol{S} + p\boldsymbol{I}, \tag{1}$$

where $\mathbf{S}$ and p are, respectively, the deviatoric tensor and the hydrostatic pressure, and $\boldsymbol{I}$ is the second order identity tensor. The hydrostatic pressure can be determined by the Eq. (2):

$$p = \frac{1}{3} tr(\boldsymbol{\sigma}), \tag{2}$$

where $tr(\boldsymbol{\sigma})$ represents the stress tensor's trace.

The relation between stress tensor and elastic strain tensor is described by the Hooke's law (Souza *et al.*, 2008), Eq. (3).

$$\boldsymbol{\sigma} = \mathbb{D}: \boldsymbol{\varepsilon^e}, \tag{3}$$

where $\mathbb{D}$ and $\boldsymbol{\varepsilon^e}$ are, respectively, a fourth order tensor called constitutive matrix and the elastic strain tensor.

Each yield function tries to describe when the plastic yielding begins. Von Mises' yield function is defined in terms of von Mises equivalent stress and initial yield stress of the material, as shown in Eq. (4).

$$\phi = q - \sigma_{y0}, \tag{4}$$

where ϕ is the von Mises yield function, σ_{y0} is the initial yield stress and q is the von Mises equivalent stress defined by the Eq. (5)

$$q = \left[\frac{3}{2} \boldsymbol{S}: \boldsymbol{S}\right]^{1/2}. \tag{5}$$

Under plastic yielding the rate of the plastic strain is determined by the plastic flow rule (Souza *et al.*, 2008), described by Eq. (6)

$$\boldsymbol{\dot{\varepsilon}^p} \equiv \dot{\gamma} \boldsymbol{N}, \tag{6}$$

where $\boldsymbol{N}$ is the so-called flow vector and $\dot{\gamma}$ is the plastic multiplier. The flow vector represents the yielding direction and is defined by Eq. (7)

$$\boldsymbol{N} \equiv \frac{\partial \phi}{\partial \sigma}. \tag{7}$$

Considering the von Mises yield function, the flow vector can be expressed by Eq. (8).

$$\boldsymbol{N} = \frac{3}{2q} \boldsymbol{S} \tag{8}$$

According von Mises isotropic-strain hardening model (Souza *et al.*, 2008), the rate of accumulated plastic strain is given by Eq. (9), and it is equal to the plastic multiplier, Eq. (10).

$$\dot{\bar{\varepsilon}}^p = \left[\frac{2}{3} \boldsymbol{\dot{\varepsilon}^p}: \boldsymbol{\dot{\varepsilon}^p}\right]^{1/2} \tag{9}$$

$$\dot{\bar{\varepsilon}}^p = \dot{\gamma} \tag{10}$$

The relation between yield stress and accumulated plastic strain can be linear or nonlinear and it is described by the hardening-strain function. In this paper the hardening-strain function, Eq. (11), will be considered as nonlinear.

$$\sigma_y = \sigma_{y0} + H(\bar{\varepsilon}^p)\, \bar{\varepsilon}^p , \tag{11}$$

where H is called the nonlinear isotropic hardening modulus. The expansion of the von Mises' yield surface represented in the pi plane can be seen in the Fig. 4.

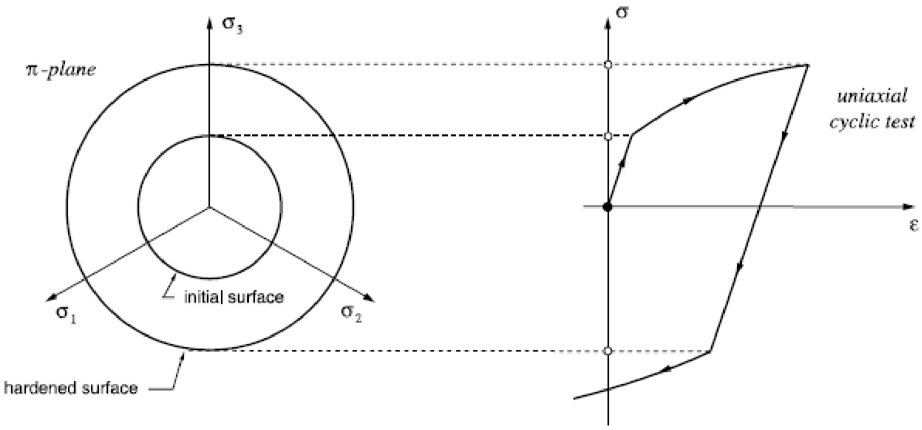

Figure 4. Isotropic hardening (Souza *et al*. 2008).

3. FINITE ELEMENT ANALYSIS

The wire frame chassis was modeled in the *SolidWorks* software using a 3D sketch tool. Once a sketch line is drawn, a structural member can be placed along that line, as shown in Fig. 5. The wire frame model was imported to the finite element software *Abaqus.*

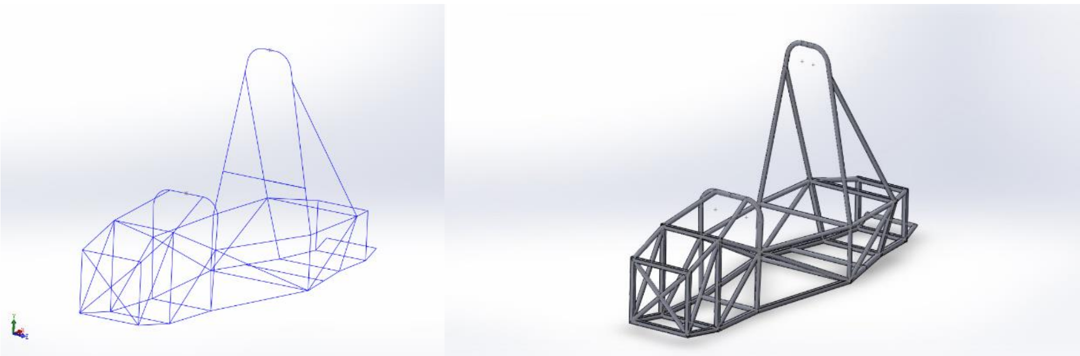

Figure 5. Wire frame chassis (left) and solid chassis (right).

Figure 6 shows the three different tubing sections used. Square tubing sections (25,4 mm x 25,4 mm) with 1.5 mm wall thickness was used to make the welding process easier, and it is shown in red. The roll hoops were made of 25,4 mm diameter and 2,4 mm thick tubes, shown in blue. The remaining tubing has 25,4 mm diameter, 1,5 mm thick and shown in yellow. The following coordinate system and labeling convention is used within this paper:

- Longitudinal (X)
- Vertical (Y)
- Transverse (Z)

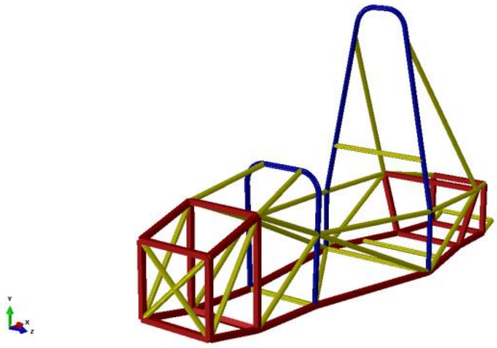

Figure 6. Tubing sections.

3.1 Finite element

A quadratic beam element with three nodes, called 'beam23', was used in the numerical analysis. The convergence study was done to determine the appropriate level of mesh refinement, aiming to find a balanced relation between results precision and computational resources. In the mesh a generic load was used, maximal von Mises equivalent stress and simulation time were compared and different levels of refinement were tested, as shown in Tab. 1. For higher levels of refinement, or smaller elements, the numerical and analytical solution should converge (Azevedo, 2003). For the studied case, the average element size was 10 mm.

Table 1. Mesh convergence.

Average element size [mm]	Number of elements	Simulation time [s]	Maximal von Mises equivalent stress [MPa]
50	641	9	409,80
25	1267	13	402,00
10	3188	21	404,50
1	31872	148	404,00

3.2 Material properties

For a proper finite element analysis it is necessary that the properties of the material used in prototype construction is determined by experimental tests or provided by the manufacturer. Since not all information was available, some properties inserted in the finite element program were taken from *MatWeb* database. It is known that the material used was a low-carbon steel AISI 1010 and estimated properties for this material are shown in Table 2.

Table 2. Material properties used in finite element analysis.

Density	76,5 kN/m³
Tensile Strength, Ultimate	360 MPa
Tensile Strength, Yield	180 MPa
Modulus of Elasticity	200 GPa
Poissons Ratio	0,29
Strain Hardening Exponent 'n'	0,21
Strength Coefficient 'K'	600 MPa

The hardening strain curve used in the elastic plastic analysis is given by Eq. (12).

$$\sigma_y = \sigma_{y0} + K\varepsilon^n \tag{12}$$

3.3 Boundary conditions

The following boundary conditions were applied on the element finite analysis.

Main Hoop:

- Load applied: *Fx = 6.0 kN*, *Fy = -9.0 kN*, *Fz = 5.0 kN*. Each load as applied separately.
- Application point: Top of Main Hoop (node 27).
- Boundary conditions: Fixed displacement (x,y,z) but not rotation of the bottom nodes of both sides of the front and main roll hoops.
- Max allowed deflection: 25 mm.

Front Hoop:

- Load applied: *Fx = 6.0 kN*, *Fy = -9.0 kN*, *Fz = 5.0 kN*. Each load was applied separately.
- Application point: Top of Front Hoop (node 36).
- Boundary conditions: Fixed displacement (x,y,z) but not rotation of the bottom nodes of both sides of the front and main roll hoops.
- Max allowed deflection: 25 mm.

3.4 Numerical results

After the finite element analysis, the nodes where von Mises equivalent stress is maximal for each load were defined and shown as red dots in Fig 7. These point represents the critical regions of the chassis, therefore are the most appropriated places for a strain gauge measurement. The blue dot (Fig. 7) shows the coordinate center. Tables 4 and 5 show the maximal deflection simulated.

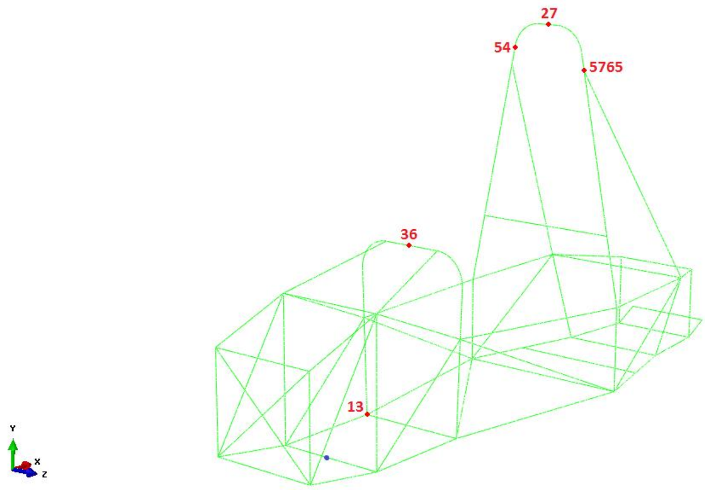

Figure 7: Critical nodes.

Table 4. Main Hoop displacements.

Main Hoop			
Loading Direction	**Longitudinal "x"**	**Vertical "y"**	**Transverse "z"**
Displacement "x" [mm]	49,1	0,79	27
Displacement "y" [mm]	6,5	1,75	119,5
Displacement "z" [mm]	2,75	1,61	336,1
Total Displacement [mm]	49,3	1,92	351,4

Table 5. Front Hoop displacements.

	Front Hoop		
Loading Direction	**Longitudinal "x"**	**Vertical "y"**	**Transverse "z"**
Displacement "x" [mm]	1,33	0,66	3,84
Displacement "y" [mm]	1,05	8,82	5,42
Displacement "z" [mm]	0,36	3,5	28,5
Total Displacement [mm]	1,33	8,84	28,6

From the results, it was verified that the displacements exceeded the maximal allowed deflection of 25 mm. The critical loads were transversal (Fy) and longitudinal (Fx) on Main Hoop and transverse load (Fy) on Front Hoop.

4. EXPERIMENTAL ANALYSIS

After FEM analysis, the structure was experimentally tested on a test bench in order to validate the numerical results. Initially, in addition of measuring the deflection, the idea was to measure all the stress critical regions pointed out in Fig. 7, but due lack of strain-gauges measurement system this stage of the experimental analysis was not executed. For deflection measurements, a coordinate measuring machine was used. All the data is collected by a computer`s software that saves the point`s coordinate before and after the load is applied.

4.1 Testing Bench

The testing bench consists of a straightening table with numerous adjustments for fixing the chassis. The table is surrounded by two gantries where hydraulic actuators can be fixed. The coordinate measurement machine (CMM) seats on a rail and has an articulated arm therefore it can reach different regions of the structure. A computer connected to the bench does the measured points acquisition. Even being designed for larger vehicles, the bench attend the requirements for the chassis testing, as shown if Fig. 8.

Figure 8. Chassis testing table

4.2 Measurement points

Due to a movement restrictor of the measuring arm, the coordinate measurement machine is incapable of measuring points below the rail line. For this reason, all selected measuring points are part of the main Hoop, as shown in Figure 9. All the selected points are symmetrical relative to the axis Y.

Points 1-5 were chosen for having presented the greatest deflections in numerical simulations and points 6 and 7 are important because they are the ends of the bar where the driver's seat belt is attached.

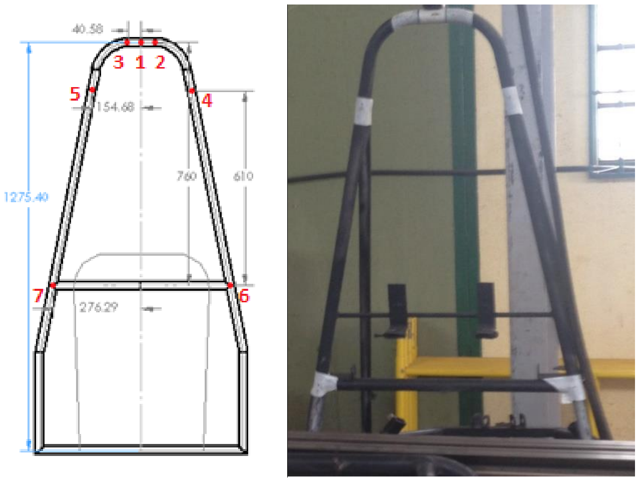

Figure 9. Measurements Points

4.3 Experimental results

The experimental displacements, U_{exp}, and displacements simulated numerically, U_{num}, are compared in Table 6. The length of the actuator was not sufficient to provide 5 kN of force for the transversal loading test, providing only 3.5 kN. Due to the Main Hoop's geometry and actuator slipping risk, the actuator was placed 150 mm below the top of Main Hoop. The data collected in this test is compared with the displacements obtained in a new simulation where the following boundary conditions were applied:

- *Fz = 5.0 kN.*
- Application point: 150 mm below the top of Main Hoop.
- Boundary conditions: Fixed displacement (x,y,z) but not rotation of the bottom nodes of both sides of the front and main roll hoops.
- Max allowed deflection: 25 mm.

Table 6. Comparing numerical and experimental results.

Loading Direction	Points	Node	U_{num} [mm]	U_{exp} [mm]	$U_{exp} - U_{num}$ [mm]
Vertical 9 kN	1	27	1,9	8,42	6,49
	2	42	1,6	8,10	6,52
	3	1	1,6	7,14	5,56
	4	40	1,5	4,82	3,32
	5	3	1,5	3,98	2,44
	6	35	0,2	4,84	4,60
	7	28	0,2	4,52	4,28
Transverse **3,5 kN**	1	27	48,3	54,55	6,26
	2	42	48,6	55,31	6,70
	3	1	48,2	54,17	5,97
	4	40	59,5	53,26	-6,19
	5	3	48,0	51,20	3,22
	6	35	15,2	20,94	5,77
	7	28	15,0	17,26	2,25
Longitudinal 6 kN	1	27	49,3	*	*
	2	42	48,5	*	*
	3	1	48,5	55,94	7,47
	4	40	10,8	13,82	3,07
	5	3	10,9	10,58	-0,29
	6	35	1,9	3,78	1,84
	7	28	1,9	6,25	4,31

The displacements indicated by "*" could not be measured due to actuator position.

5. CONCLUSIONS

The conclusion of the various simulations made was that the chassis does not have the necessary stifiness stipulated by the FSAE rules under longitudinal and transverse loads on the Main hoop and transverse load on the Frons Hoop. As a solution to the chassis stiffness problem, it is suggested to change the geometry of the prototype, adding or repositioning bars. The new geometry was simulated under the three critical loads, and it has shown to be rigid enough, as shown in Table 7.

Table 7: Max deflections of the modified geometry.

		Max Deflections [mm]	
Loading Direction	Application point	Original Geometry	Modified Geometry
Transverse 5,0 kN	Main Hoop	351,4	6,34
Longitudinal 6,0 kN	Main Hoop	49,3	12,7
Transverse 5,0 kN	Front Hoop	28,6	24,5

The numerical analysis was also satisfactory in determining displacements at points on the main Hoop, since all simulated displacements did not differ more than 7.5 mm from the experimental values.

The bench tests is suitable for the type of experiment performed in this work, however it is necessary special care to attach the chassis to the testing bench.

6. REFERENCES

Azevedo, A.F.M. *Método dos elementos finitos.* 1. Ed. Porto: Universidade do porto, 2003.

MILLIKEN W.F.; MILLIKEN, D. L.; 1995. *Race Car Vehicle Dynamics.* Warrendale: Society Of Automotive Engineers.

SAE International, *2014 FSAE Rules*, http://students.sae.org/cds/formulaseries/rules/2014_fsae_rules.pdf - 10/06/2014.

De Souza Neto, E.A., Peri´c, Owen, D.R.J., *Computational methods for plasticity: theory and applications*, 2008.

Venâncio N. F. *Projeto do chassi de uma viatura de formula*, Thesis of the integrated master's degree in mechanical engineering: Universidade do Porto, June 2013.

7. RESPONSIBILITY NOTICE

The author are the only responsible for the printed material included in this paper.